

Supplementary Information

Synthetic conversion of a graded receptor signal into a tunable, reversible switch

Santhosh Palani¹ and Casim A. Sarkar^{1,2,3}

¹Department of Bioengineering, ²Department of Chemical & Biomolecular Engineering, University of Pennsylvania, Philadelphia, Pennsylvania 19104-6321 USA

³Author to whom correspondence should be addressed

240 Skirkanich Hall, 210 S. 33rd Street

Department of Bioengineering, University of Pennsylvania

Philadelphia, PA 19104-6321

Tel: 215-573-4072

Fax: 215-573-2071

E-mail: casarkar@seas.upenn.edu

Contents

Supplementary Text.....	S1
Figure S1. Interconnected, linear positive feedback loops can convert a hyperbolic response into a switch-like response.....	S6
Figure S2. Single-cell fluorescence distributions during temporal deactivation	S7
Figure S3. Decoupling ultrasensitivity and steady-state setpoint	S8
Table S1. Differential equations and dimensionless initial conditions for the model in Figure 1	S9
Table S2. Dimensionless rate constants for the model in Figure 1	S10
Table S3. Plasmids used in this study	S11
Table S4. Yeast strains used in this study	S11
Model Source Files	S12

Supplementary Text

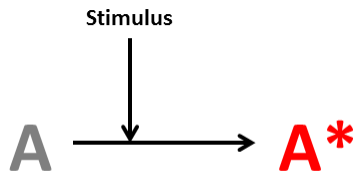
Interconnected, linear positive feedback loops can generate bistability

It has previously been shown that cooperative feedback loops can generate a bistable response. Here, we show that two interconnected, but linear, positive feedback loops can also generate bistability. To show how this topology can mimic cooperative feedback, we simulated stimulus-induced activation of a one-component system with different topological connections.

First, we introduce the basal network which contains no feedback processes (Topology 1). Then, we extend Topology 1 by introducing a single feedback loop in either stimulus-induced activation (Topology 2) or synthesis (Topology 3). Finally, we integrate Topologies 2 and 3 to derive the one-component analog (Topology 4) of the network presented in the main text (Figure 1A).

Topology 1: Basal topology yields a purely hyperbolic activation response

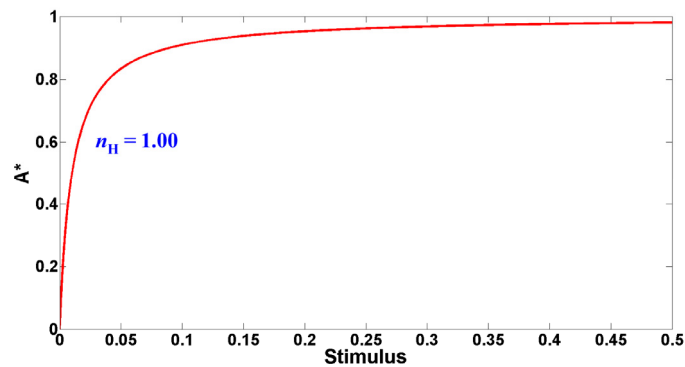
Mechanism: Species A is produced at a basal rate B^A . External stimulus activates species A to A^* . Steady state is achieved through first-order degradation of A and A^* . A_{tot} , which is the sum of A and A^* , remains constant in the absence of synthesis feedback.



Dynamics:

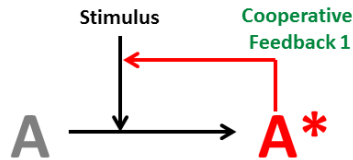
$$\frac{dA^*}{dt} = stimulus(A_{tot} - A^*) - k_{deg} A^*$$
$$\frac{dA_{tot}}{dt} = B^A - k_{deg} A_{tot}$$

Steady-state response: The activated species A^* shows a truly graded response (Hill coefficient (n_H) = 1.00) with change in stimulus.



Topology 2: Bistability through stimulus-enhancing feedback requires cooperativity

Mechanism: We can modify Topology 1 by introducing a ‘self-activating’ positive feedback through the external stimulus (f_1 term in the equation). Unlike Topology 1, this network can generate bistability as long as the feedback is cooperative ($m > 1$). When the feedback is linear ($m = 1$), the system only shows mild ultrasensitivity and remains monostable.

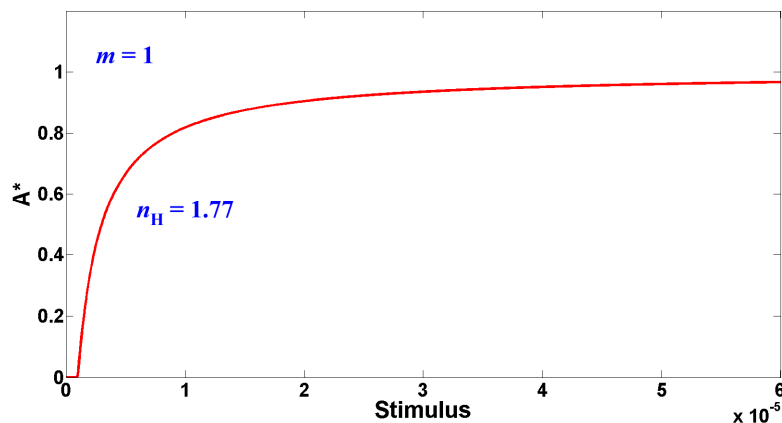
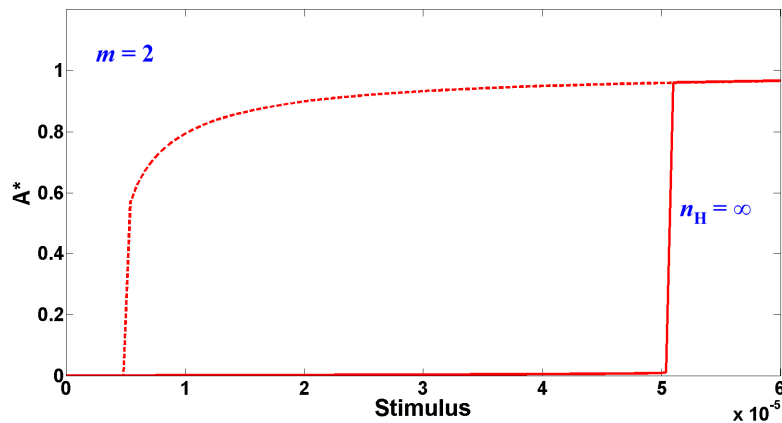


Dynamics:

$$\frac{dA^*}{dt} = stimulus(A_{tot} - A^*) \left[1 + \frac{f_1(A^*)^m}{K_1^m + (A^*)^m} \right] - k_{deg} A^*$$

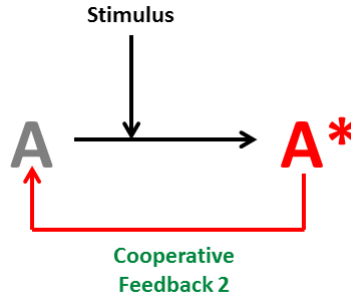
$$\frac{dA_{tot}}{dt} = B^A - k_{deg} A_{tot}$$

Steady-state response: To achieve a bistable response, m has to be greater than 1 (here, $m = 2$).



Topology 3: Bistability through synthesis feedback requires cooperativity

Mechanism: We can alternatively modify Topology 1 to introduce feedback to synthesize more inactive species A (f_2 term in the equation). Similar to Topology 2, this network can generate bistability when the feedback is cooperative ($m > 1$) but it shows only mild ultrasensitivity with linear feedback ($m = 1$).

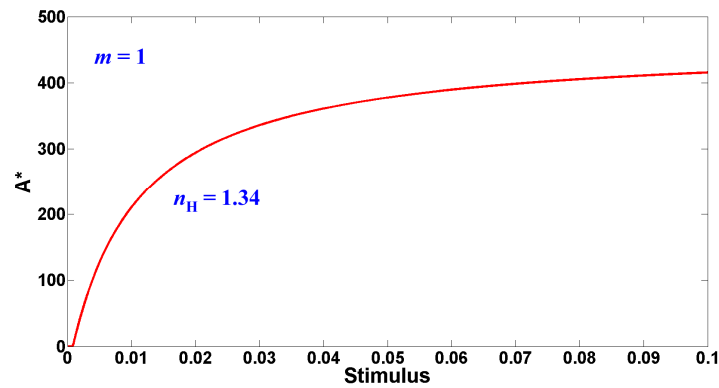
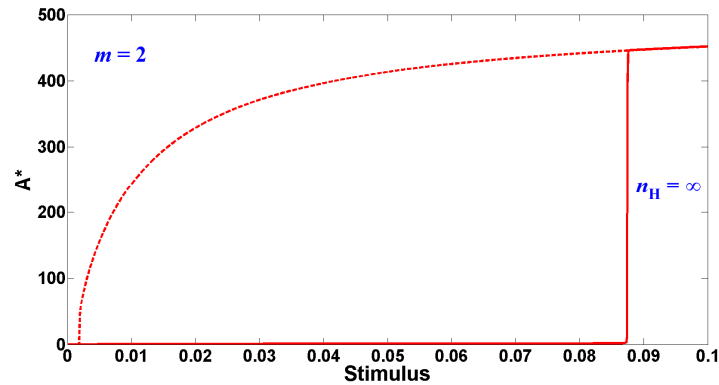


Dynamics:

$$\frac{dA^*}{dt} = stimulus(A_{tot} - A^*) - k_{deg}A^*$$

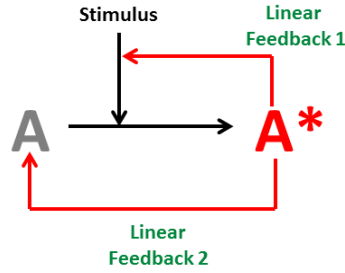
$$\frac{dA_{tot}}{dt} = B^A - k_{deg}A_{tot} + \frac{f_2(A^*)^m}{K_2^m + (A^*)^m}$$

Steady-state response: To achieve a bistable response, m has to be greater than 1 (here, $m = 2$).



Topology 4: Bistability through both stimulus-enhancing and synthesis feedbacks can be achieved without cooperativity

Mechanism: We can now derive the topological analog of the network used in the paper (Figure 1A) by combining the two feedback loops in Topologies 2 and 3. In contrast to these two previous topologies, Topology 4 can exhibit bistability without cooperativity in either feedback loop ($m = 1$). Thus, this network architecture, in which two linear feedbacks interconnect in the generation of A^* , can mimic cooperative feedback, and thereby achieve bistability, without any explicit molecular requirements for cooperativity.

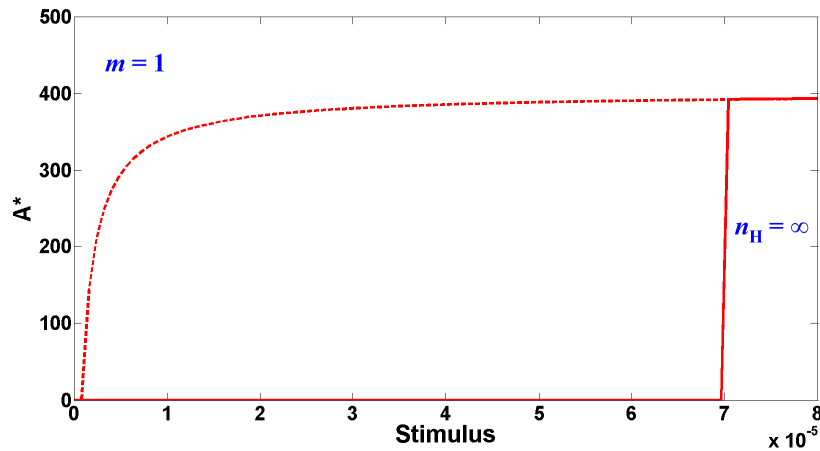


Dynamics:

$$\frac{dA^*}{dt} = stimulus(A_{tot} - A^*) \left[1 + \frac{f_1(A^*)^m}{K_1^m + (A^*)^m} \right] - k_{deg} A^*$$

$$\frac{dA_{tot}}{dt} = B^A - k_{deg} A_{tot} + \frac{f_2(A^*)^m}{K_2^m + (A^*)^m}$$

Steady-state response: Unlike the previous topologies, a bistable response can be achieved with $m = 1$.



Parameters used for steady-state response plots in Topologies 1-4:

Common parameters:

$$B^A = 0.01, k_{deg} = 0.01$$

Initial conditions:

$$A_{tot} = 1, A^* = 0$$

Topology 2:

$$f_1 = 10000, K_1 = 1$$

Topology 3:

$$f_2 = 5, K_2 = 40$$

Topology 4:

$$f_1 = 10000, K_1 = 100, f_2 = 5, K_2 = 100$$

Figure S1. Interconnected, linear positive feedback loops can convert a hyperbolic response into a switch-like response

The topology with two interconnected, linear positive feedback loops (Figure 1A) is sufficient to convert a hyperbolic response into a switch. The basal signaling pathway, without either feedback, consists of the minimum components that connect a cell-surface signal to transcription factor activation. This basal network does not have any known sources of ultrasensitivity, including cascading, multi-step activation, zero-order ultrasensitivity, or molecular cooperativity. Therefore, as expected, the basal network exhibits a truly hyperbolic response (Hill coefficient (n_H) = 1.00). When only receptor feedback is added, a small level of ultrasensitivity is achieved (n_H = 1.34 for R_s = 3); similarly, with only transcription-factor feedback, the Hill coefficient increases modestly (n_H = 1.86 for TF_s = 3). Thus, neither feedback loop in isolation is sufficient for generating a strongly ultrasensitive or bistable output. However, when both feedbacks are added to the basal network, the response is a true bistable switch.

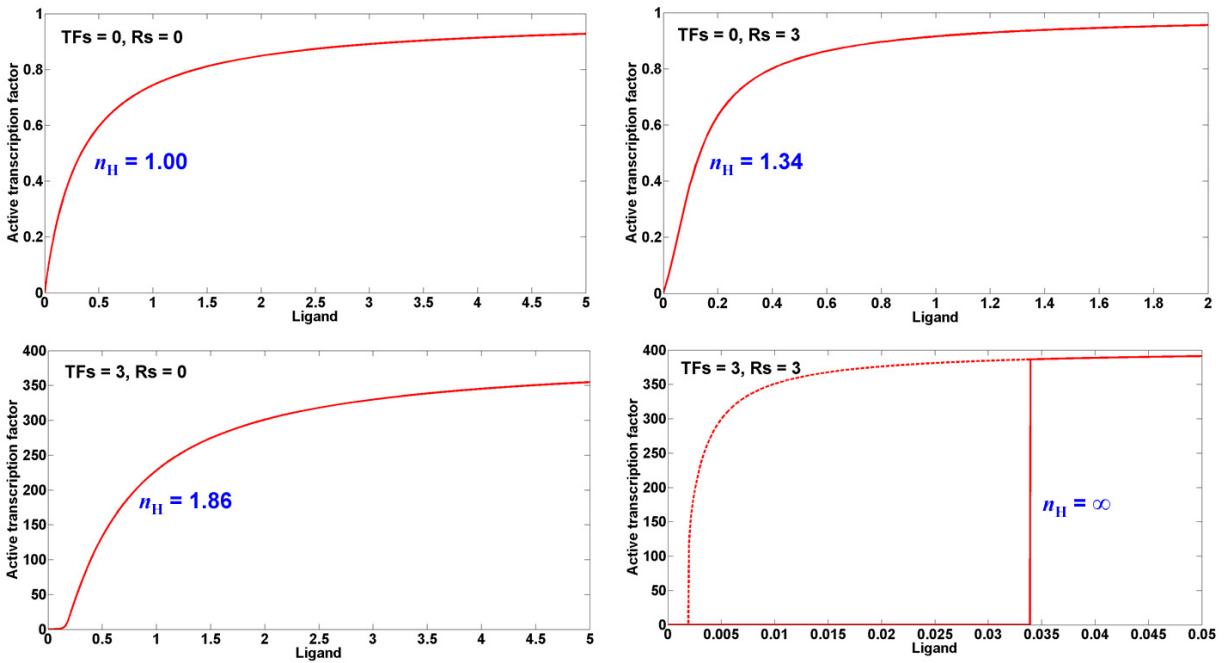


Figure S2. Single-cell fluorescence distributions during temporal deactivation

Naïve cells (cRcTF or tRtTF) stimulated with 0.06 μM IP remain inactive after 24 hours (top row), whereas naïve cells stimulated with 1 μM IP show full activation after 24 hours (second row). After fully activating cRcTF and tRtTF cells in 1 μM IP, the cells were then switched to media containing a sub-threshold concentration of IP (0.05 μM). The entire population of monostable cRcTF cells becomes less fluorescent over time (left column, bottom four panels); by contrast, the fluorescence distribution of the bistable tRtTF population becomes highly bimodal over time, with the ‘on’ population having the same mean fluorescence as fully activated cells in 1 μM IP (right column, bottom four panels). The small peak observed at 12 hours (0.05 μM IP) in the tRtTF strain is not an ‘off’ population but cell debris, as very high levels of SKN7 can be toxic. The cells were spun down and washed at 12 hours to remove this debris which is why this peak is not seen at 24 hours (0.05 μM IP).

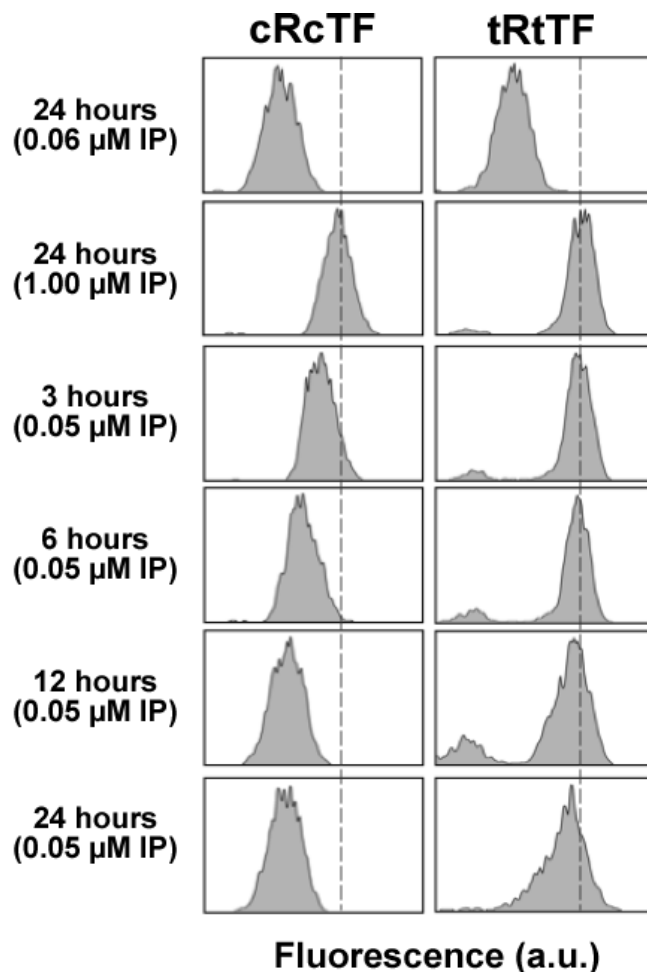


Figure S3. Decoupling ultrasensitivity and steady-state setpoint

Ultrasensitivity and steady-state setpoint can be decoupled by varying the strength of the constitutive TF promoter or the TF feedback promoter. In our model, the constitutive TF promoter strength can be altered through the basal rate of synthesis of I (B^I) and the TF feedback promoter strength can be tuned through the feedback strength to I (TFs). As seen in the simulations below, variable setpoint and low ultrasensitivity can be achieved by changing B^I in the cRcTF strain; similarly, variable setpoint and high ultrasensitivity can be obtained by changing TFs when Rs is strong (i.e., when the strain is transcription factor-limited).

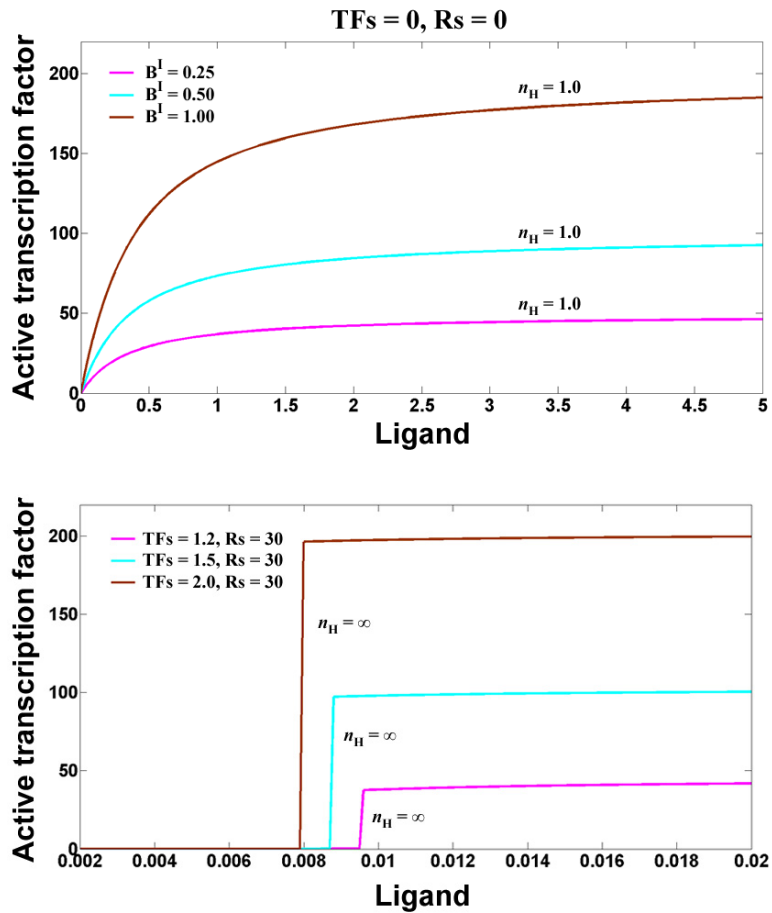


Table S1. Differential equations and dimensionless initial conditions for the model in Figure 1

Species	Description	Differential equation	Initial condition
L	Ligand	N/A (held constant)	N/A (stimulus)
R	Receptor	$\frac{dR}{dt} = B^R - k_{degR}R - k_{on}LR + k_{off}C + \frac{R_S A}{K_D + A}$	$R_0 = 1$
C	Ligand-Receptor Complex	$\frac{dC}{dt} = k_{on}LR - k_{off}C - k_{degC}C - k_1CI + (k_2 + k_3)X$	$C_0 = 0$
I	Inactive Transcription Factor	$\frac{dI}{dt} = B^I - k_{degI}I - k_1CI + k_2X + \frac{TF_S A}{K_D + A}$	$I_0 = 1$
X	C bound to I	$\frac{dX}{dt} = k_1CI - (k_2 + k_3)X - k_{degX}X$	$X_0 = 0$
A	Active Transcription Factor	$\frac{dA}{dt} = k_3X - k_{degA}A$	$A_0 = 0$

Table S2. Dimensionless rate constants for the model in Figure 1

Rate constant	Description	Value
B^R	Basal synthesis of R	0.005
k_{degR}	Degradation rate of R	0.005
k_{on}	Association rate constant for L and R	0.001
k_{off}	Dissociation rate constant for C	0.05
R_S	Strength of R feedback	3
K_D	Michaelis constant for synthesis of R and I by A	200
k_{degC}	Degradation rate of C	0.01
k_1	Association rate constant for C and I	1
k_2	Dissociation rate constant for X	5
k_3	Activation rate constant for A	45
B^I	Basal synthesis of I	0.005
k_{degI}	Degradation rate of I	0.005
TF_S	Strength of I feedback	3
k_{degX}	Degradation rate of X	0.005
k_{degA}	Degradation rate of A	0.005

Table S3. Plasmids used in this study

Plasmid	Properties	Reference
pRS403	HIS3, integration vector	Stratagene
pRS405	LEU2, integration vector	Stratagene
DQ232595	CEN6/ARSH4, HIS3, P _{SSRE} -yEGFP3-T _{ADHI}	(1)
DQ232596	CEN6/ARSH4, HIS3, P _{TR-SSRE} -yEGFP3-T _{ADHI}	(1)
DQ232600	CEN6/ARSH4, LEU2, P _{CYCI} -AtCRE1a, P _{SSRE} -yEGFP3-T _{ADHI}	(1)
pSP001	LEU2, P _{CYCI} -AtCRE1a, P _{SSRE} -yEGFP3-T _{ADHI}	This study
pSP002	LEU2, P _{SSRE} -AtCRE1a, P _{SSRE} -yEGFP3-T _{ADHI}	This study
pSP003	LEU2, P _{TR-SSRE} -AtCRE1a, P _{SSRE} -yEGFP3-T _{ADHI}	This study
pSP004	HIS3, P _{TR-SSRE} -SKN7-T _{ADHI}	This study

Table S4. Yeast strains used in this study

Yeast Strain	Properties	Reference
TM182	MAT leu2 his3; sln1::hisG; P _{GAL1} -PTP2 (ura3)	(2)
cRcTF	TM182 + pSP001 (leu2)	This study
sRcTF	TM182 + pSP002 (leu2)	This study
tRcTF	TM182 + pSP003 (leu2)	This study
cRtTF	cRcTF + pSP004 (his3)	This study
sRtTF	sRcTF + pSP004 (his3)	This study
tRtTF	tRcTF + pSP004 (his3)	This study

References

1. Chen MT, Weiss R (2005) Artificial cell-cell communication in yeast *Saccharomyces cerevisiae* using signaling elements from *Arabidopsis thaliana*. *Nat Biotechnol* **23**: 1551-1555
2. Maeda T, Wurgler-Murphy SM, Saito H (1994) A two-component system that regulates an osmosensing MAP kinase cascade in yeast. *Nature* **369**: 242-245

Model Source Files

The model for Figure 1 (given in Tables S1 and S2) is also available in SBML format (see separate supplementary file) and in the BioModels Database (<http://www.ebi.ac.uk/biomodels/>; accession number MODEL1102160000).